Food and Bioprocess Technology (2023) 16:368–381
https://doi.org/10.1007/s11947-022-02944-8

RESEARCH

Microencapsulation of Rose Essential Oil Using Perilla Protein Isolate-Sodium Alginate Complex Coacervates and Application of Microcapsules to Preserve Ground Beef

Liqing Qiu[1,3] · Min Zhang[1,2] · Benu Adhikari[4] · Lu Chang[5]

Received: 27 July 2022 / Accepted: 6 November 2022 / Published online: 11 November 2022

Abstract

Rose essential oil (REO) microcapsules were prepared using perilla protein isolate (PPI)-sodium alginate (NaAlg) complex coacervates as shells. PPI-to-NaAlg ratio of 6:1 and pH 3.8 were the optimum parameters for obtaining PPI-NaAlg coacervates. The multicore morphology and large particle size of microcapsules indicated the successful encapsulation of REO in PPI-NalAg shells. The hydrogen bond between the core and wall and electrostatic interaction between PPI and NaAlg were confirmed by Fourier-transform infrared (FTIR) spectra. The encapsulation efficiency, payload, and encapsulation yield of the microcapsules were 89.80%, 53.17%, and 88.26%. Additionally, the microencapsulated REO displayed better thermal stability and sustained-release profile than free REO. Microencapsulation of REO in PPI-NaAlg shell matrix improved its antibacterial ability. Incorporation of REO microcapsules in ground beef increased its shelf life by 6 days at 4 ℃. Encapsulation of REO in the PPI-NaAlg coacervates may be simple and effective way for improving its preservative effects on meat.

Keywords Rose essential oil · Microcapsules · Perilla protein · Complex coacervate · Ground beef · Preservation

Introduction

Meat and meat products are excellent resources of macro and micronutrients such as protein, phosphorus, iron, vitamin B12, and zinc. However, fresh meat is perishable, and its shelf life is limited to about 1 week at 4 ℃ due to the microbial contamination and oxidative deterioration (Smaoui et al., 2021). Because of the increased contact area between meat fat and oxygen, and the higher availability of oxidation promoters, relatively rapid oxidation occurs in ground meat products (Rodrigues Arruda et al., 2022). Therefore, shelf-life extension of meat products by inhibiting the microbial spoilage and oxidation are import considerations in meat industry.

Rose essential oil (REO) has been traditionally used in cosmetics and medical products for its pleasant rosy scent and pharmacological properties, respectively (antitussive, anti-inflammatory and antidiabetic effects) (Ulusoy et al., 2009). Recently, several research works have shown that REO possesses antibacterial (Ulusoy et al., 2009), antifungal (Mahajan & Pal, 2020), and antioxidant capacities (Liu et al., 2021). These properties make REO a potential option for meat preservation. However, several limitations of REO such as poor stability, high hydrophobicity and volatility have hindered its greater application as a food preservative (Liu et al., 2021).

Complex coacervation–based microencapsulation method is found to be suitable for the microencapsulation of many active and hydrophobic substances (Gomez-Estaca et al., 2018). It can provide a controlled release profile and chemical stability of the encapsulated compounds, prevent the interaction of additives with food ingredients, and hinder the undesirable flavor of the core materials (da Silva Soares

✉ Min Zhang
min@jiangnan.edu.cn

1 State Key Laboratory of Food Science and Technology, Jiangnan University, Wuxi, Jiangsu 214122, China

2 Jiangsu Province International Joint Laboratory On Fresh Food Smart Processing and Quality Monitoring, Jiangnan University, Wuxi, Jiangsu 214122, China

3 China General Chamber of Commerce Key Laboratory On Fresh Food Processing & Preservation, Jiangnan University, Wuxi, Jiangsu 214122, China

4 School of Science, RMIT University, Melbourne VIC3083, Australia

5 Shandong Huamei Biology Science & Technology Co, Pingyin, China

et al., 2021; Karagozlu et al., 2021; Tavares et al., 2019). Gelatin is the most extensively used protein source in the complex coacervation process of lipophilic/hydrophilic compounds such as thyme essential oil (Göktepe et al., 2021), roasted coffee oil (Zanin et al., 2021), anthocyanins (Stănciuc et al., 2017), and oregano oil (Karagozlu et al., 2021). Nevertheless, gelatin must be heated to dissolve in water before use but agglomerated at ambient temperature, which increased the operation difficulty of complex coacervation based on gelatin (Gomez-Estaca et al., 2018). Additionally, glutaraldehyde, the commonly used cross-linking agent of gelatin-based system, can create damage to human health (Stănciuc et al., 2017). Consequently, other animal proteins and plant proteins have been explored as alternatives to gelatin as shell materials in complex coacervation-based microencapsulation technologies (Misra et al., 2022). Milk proteins and egg proteins are another two widely explored animal proteins to produce coacervates. For example, da Silva Soares et al. (2021) used ovalbumin and pectin as the wall materials for the microencapsulation of sacha inchi oil by complex coacervation. Recently, Tavares and Noreña (2020) and Tavares et al. (2019) employed whey protein/gum Arabic and whey protein/chitosan to study their encapsulation effects on ginger essential oil and ginger extract, respectively. However, the higher allergenic nature of these two animal proteins compared to plant proteins (except for a few plant proteins such as gluten and peanut protein) hindered their application in various food systems (Jawanda et al., 2022). Due to the healthier nature and increased popularity of plant proteins, new plant proteins should be explored for the microencapsulation of REO to expand the applicability and scope of this technology.

Perilla protein isolate (PPI) is a by-product of perilla oilseed processing. PPI has high nutritive value, balanced amino acid composition, and superior protein efficiency, and thus it can be considered an alternative source of animal protein (Zhao et al., 2021a, b). Besides, PPI possessed a high emulsifying activity and emulsion stability; both of which are desirable properties of the wall materials used for microencapsulation (Zhao et al., 2021a, b). Nevertheless, the researches on PPI are mainly focused on extraction and modification (Yang et al., 2022). The application of PPI as a wall material to prepare microcapsules containing bioactive substances (e.g., essential oil) has not been reported yet. Sodium alginate (NaAlg) is a polysaccharide with negative charge extracted from brown algae. It comes with advantages in terms of biodegradability, water solubility, non-toxicity, and resistance to oral and gastric digestion making it an ideal encapsulating shell material. Furthermore, alginate can bind divalent cations and produce a hexagonal lattice which is known as an "egg-box" gel structure (Jadach et al., 2022). Colloidal delivery systems containing sodium alginate rapidly increase the viscosity upon contact with body environment which is advantageous for targeted sustained release (Jadach et al., 2022). According to the literature, NaAlg is commonly used for the preparation of hydrogel beads to encapsulate essential oils, such as clove essential oil (Faidi et al., 2019), *Ziziphora clinopodioides-Rosmarinus officinalis* essential oil (Karimifar et al., 2022), and lemongrass essential oil (Salvia-Trujillo et al., 2013). However, the NaAlg-based capsules are instable in the release media due to the leaching of Ca when it complexes with other molecules and/or due to salt exchange (Matricardi et al., 2008). In addition, the high porosity of the beads usually leads to a burst effect or to uncontrolled active principle release (Matricardi et al., 2008). Nowadays, complex coacervation of NaAlg with oppositely charged polymers to prepare essential oil loaded microcapsules has been reported for gelatin (Bastos et al., 2020a, b, c), lactoferrin (Bastos et al., 2020a), and whey protein (Bajac et al., 2022). As reported, microcapsules prepared via complex coacervation displayed high thermal and oxidation stability (Faidi et al., 2019). Additionally, the controlled release of core materials from microcapsules can also be achieved via this technique (Bajac et al., 2022). However, there is no study that has elaborated the complex coacervation process between PPI and NaAlg and used these complex coacervates as wall material to encapsulate REO. In addition, the freshness-keeping effects of REO and REO microcapsules on the meat products have also not been investigated.

This work focused on the feasibility of using PPI-NaAlg complex coacervates for the encapsulation process of REO. It involves characterization of microcapsules with REO (particle diameter, morphology, structure, thermal characteristic), the measurements of REO release profile in model foods, and the determination of bacteriostatic effects of REO microcapsules. The freshness-keeping effects of REO microcapsules on ground beef were investigated as well.

Materials and Methods

Materials

Perilla seeds were purchased from Huannan Zisuyuan Technology Development Co., LTD. (Heilongjiang, China). Rose essential oil (REO) was obtained from Huamei Biotechnology Co., Ltd. (Shandong, Pingyin, China). Freshly ground beef (immediately after grounding) was brought from a local China Resources Vanguard Supermarket in Wuxi. NaAlg (purity ≥ 90%, β-D-mannuronic/α-L-guluronic = 0.51), acetic acid (CH_3COOH), hydrochloric acid (HCl), n-hexane, sodium hydroxide (NaOH), ethanol, potassium bromide (KBr), trichloroacetic acid, trichloromethane, methyl red, MgO, boric acid (H_3BO_3), and potassium bromophenol green were of analytical level and were obtained from Beijing Innochem Science & Technology Co., LTD. (Beijing, China).

Extraction of Perilla Protein Isolate

The extraction of perilla protein isolate (PPI) was performed according to Zhao et al. (2021a, b) with slight modification. In brief, perilla seeds were milled using a household grinder (M150A, Baijie, China) for 5 min. The ground perilla seeds were defatted with n-hexane for 2 h, and the procedure was repeated 3 times. One hundred grams of the defatted flour and 1000 mL distilled water were mixed thoroughly, and the mixture was alkalized to pH 9.0. Then, the mixed suspension was stirred at 50 ℃ for 1 h, followed by centrifugation (5600 × *g*, 20 min). Subsequently, the pH of the supernatant obtained was adjusted to 4.5 with CH_3COOH solution, and the precipitate was gathered by centrifugation (5600 × *g* for 20 min). The precipitate was washed with deionized water for five times. The PPI obtained in this way was freeze dried and kept at – 18 ℃ until used. The contents of protein, moisture, fat, and ash of the PPI obtained in this way were 87.95 ± 3.64%, 4.34 ± 0.23%, 1.34 ± 0.02%, and 1.91 ± 0.43%, respectively.

Preparation of PPI and NaAlg Stock Solutions

PPI (2%, w/v) solution was produced by dissolving the lyophilized PPI in distilled water followed by stirring at 800 rpm for 45 min at ambient temperature (25 ℃). The PPI solution was alkalized to pH 9.0 via NaOH (0.001–0.1 M) and stirred for 3 h to facilitate hydration, followed by acidizing the solution to pH 7 with 0.01–1 M CH_3COOH solution. Gentle stirring was maintained for another 12 h using a magnetic stirrer to ensure complete dissolution. This PPI solution was subjected to centrifugation (5520 × *g* for 15 min) again to remove insoluble components. A fraction of PPI stock solution was thoroughly freeze dried to calculate the true protein concentration, and the result was 1.62 ± 0.07% (w/v). NaAlg stock solution (1%, w/v) was produced by dissolving the powdered NaAlg in deionized water by mechanically stirring at 600 rpm for 12 h. The pH of NaAlg solution was adjusted to pH 7 with 0.01–1 M CH_3COOH. Both PPI and NaAlg stock solutions were kept at 4 ± 1 ℃ until used.

Measurement of Turbidity

A UV-8000A spectrophotometer (Metash Instruments Co., LTD, Shanghai, China) was applied to test the turbidity of the PPI/NaAlg mixtures with different mixing ratios at 600 nm with pH ranging from 2.0 to 7.0. The concentration of the total biopolymer solid was fixed at 0.05% (w/v).

Measurement of Zeta Potential

The values of zeta potential of PPI, NaAlg, and the mixtures of these two molecules (0.05%, w/v) at different mixing ratios (PPI/NaAlg) were determined as a function of pH value (2.0–7.0) by a Zetasizer (NANOTRAC WAVE II, Microtrac MRB, USA). Experiments were carried out at 25 ℃, and the refractive index of dispersed phase was 1.59.

Measurement of the Yield of Complex Coacervates

The yield of PPI-NaAlg complex coacervates produced at various PPI to NaAlg ratios was measured based on the method as previously described by Plati et al. (2021). Generally, the pH of these mixtures was acidified to the optimal values indicated by the highest turbidity. The precipitate was gathered and freeze dried after centrifugation (5600 × *g*, 20 min). The yield of complex coacervate was measured using the equation listed as follows:

$$C_y = \frac{M_c}{M_{PPI} + M_{NaAlg}} \times 100\% \quad (1)$$

where M_c, M_{PPI}, and M_{NaAlg} represent the mass (g) of PPI-NaAlg complex coacervate, PPI, and NaAlg, respectively.

Fabrication of PPI-NaAlg Coacervates and REO Microcapsules

PPI-NaAlg complex coacervates were prepared on the basis of Chen et al. (2021) with some modifications. One percent (w/v) of PPI solution was mixed with 1% (w/v) NaAlg solution with a ratio of 6:1. This ratio was chosen based on the optimum conditions for the formation of complex coacervates. Subsequently, the mixture was acidified to pH 3.8 using CH_3COOH solution under constant stirring (300 rpm). The temperature of the mixture was lowered to 4 ℃ and then stirred further at 150 rpm for 30 min. The mixture was refrigerated at 4 ℃ for 24 h.

The fabrication of REO loaded microcapsules was carried out as proposed by Santos et al. (2021) with some minor modifications. REO emulsion was firstly produced by mixing REO with PPI-NaAlg solution (REO:PPI-NaAlg = 1.5:1.0) and homogenizing by a high pressure homogenizer (Nano-Genizer20K, Genizer, USA) at 10,000 rpm for 5 min. Subsequently, the pH of the mixture was adjusted to 3.8 with stirring (300 rpm), followed by stirring (150 rpm) at 4 ℃ for another 30 min. After refrigerating at 4 ℃ for 24 h, the PPI-NaAlg coacervates and microcapsules containing REO were freeze dried and kept at 4 ℃ until analyzed.

Measurement of Particle Size and Microscopy

A laser particle diameter analyzer (PSA 1190, Anton Paar, Austria) was used to perform the measurements of particle size of the liquid REO microcapsules and coacervates

before lyophilization. The samples were dispersed evenly into the wet dispersion sample tank of the analyzer for determination (Plati et al., 2021). The images of PPI-NaAlg coacervates and microcapsules with REO were obtained by an inverted fluorescence Microscope (Axio Vert A1, Carl Zeiss, Oberkochen, Germany) at 200 × magnification.

Measurement of Encapsulation Efficiency, Payload, and Encapsulation Yield

The total oil (TO) and surface oil (SO) contents of the prepared lyophilized microcapsules containing REO were calculated as previously reported (Bakry et al., 2019). Generally, 1.5 g of microcapsules with REO were mixed with 150 mL ethanol in a beaker (100 mL). The SO content of REO microcapsules was determined via slightly shaking the breaker for several times, followed by filtration using filter paper (Whatman No.1). The SO content was determined by the supernatant obtained. The TO content of REO was extracted by ultrasound sonication at 40 ℃ for 30 min, followed by centrifugation (10,000 × *g*, 20 min) at ambient temperature. The residues were washed using anhydrous ethanol for 3 times, and the supernatant was collected and used for the calculation of the TO content of REO microcapsules. The REO content in the ethanolic solution was determined at absorbance of 230 nm using a spectrophotometer. The oil content of REO was calculated using a standard curve. The encapsulation efficiency (EE), payload (PL), and encapsulation yield (EY) of the prepared microcapsules with REO were measured applying Eqs. (2), (3), and (4), respectively:

$$EE\ (\%) = \frac{W_t - W_s}{W_t} \times 100 \tag{2}$$

$$PL\ (\%) = \frac{W_t}{W_2} \times 100 \tag{3}$$

$$EY\ (\%) = \frac{W_t}{W_1} \times 100 \tag{4}$$

where W_t and W_s represent the weight (g) of TO and SO of REO microcapsules. W_1 and W_2, represent the weight (g) of REO used microencapsulation and the weight (g) of the microcapsules, respectively.

Measurement of Molecular Interaction by FTIR

The structure of and molecular interaction among components of samples (PPI, NaAlg, REO, PPI-NaAlg coacervates, and microcapsules with REO) were carried out based on the approach of Ren et al. (2019) using a FTIR spectrometer (IS10, Nicolet, USA). Each sample was determined at a range of wavenumber from 4000 to 400 cm^{-1}. The resolution and scanning speed of the FTIR test was set as 4 cm^{-1} and 0.2 cm/s, respectively.

Measurement of Thermal Stability

A thermal gravimetric analyzer (TGA2, Mettle Toledo Instruments, Switzerland) was used to perform the thermogravimetric analysis (TGA) of free REO, PPI-NaAlg coacervates, and microcapsules containing REO. Approximately 2 mg of the test sample was used for analysis, and the change or loss of mass was recorded ranging from 25 to 500 ℃. The heating rate was set as 10 ℃/min, and the nitrogen gas (20 mL/min) was used as the medium for heating process.

Measurement of Release Characteristics in Different Food Simulants

The REO release kinetics in different food media including deionized water, 3% acetic acid, and 10% and 50% anhydrous ethanol were studied to simulate the release characteristics of REO microcapsules in aqueous, alcoholic, oily, and acidic food systems according to Chen et al. (2021). Specifically, 20 mg of REO microcapsule samples were added into 50 mL of the abovementioned model fluid solution and stirred at 25 ℃ (100 rpm). The released REO from REO microcapsules was analyzed through determining the absorbance of the solution at wavelength of 230 nm at proper time intervals.

To further investigate the release mechanism of REO from microcapsules to different food simulants, Weibull's Eq. (5) is used for data fitting (Macheras & Dokoumetzidis, 2000):

$$\frac{M_t}{M_\infty} = 1 - \exp(-\alpha t^\beta) \tag{5}$$

where $\frac{M_t}{M_\infty}$, α, and β represent released fraction of REO, scale parameter, and shape parameter, respectively.

Measurement of the Growth Behavior of E. coli and S. aureus in the Presence of REO and REO Microcapsules

The growth curves of *E. coli and S. aureus* was determined according to Bansal et al. (2021) with proper modification. Generally, 50 μL of the cultured bacterial suspension (10^6 CFU/mL) was added into 50 mL broth followed by adding REO (1.00 mg/mL) or REO (1.88 mg/mL) microcapsules and incubated at 37 ℃ for 24 h. The optical density (OD_{600}) values of these samples were determined at 2 h interval.

Preservative Effect of REO Microcapsules on Ground Beef During Storage

Treatment of Beef Sample

The ground beef samples (pH 5.6) were prepared into 3 groups: neat ground beef (control), beef samples containing 0.40% (w/w) REO, and beef samples containing 0.75% (w/w) REO microcapsules (calculated from the payload value of REO microcapsules). These samples were sealed into polyethylene bags and stored at 4 ℃ in a refrigerator for until analyzed.

Measurement of Total Bacterial Count

The total bacterial count (TBC) was measured according to Sun et al. (2021). Briefly, 10 g of the above-mentioned ground beef samples were homogenized with 90 mL of normal saline (0.85%, w/v). The agar plate method was used to measure TBC after culturing at 37 ℃ for 48 h.

Measurement of TVB-N Value

The total volatile basic nitrogen (TVB-N) value of beef samples was determined according to Liu et al. (2020) using semimicro-Kjeldahl method. After 6 min of distillation, the distillate was titrated with HCl solution (0.01 M), and the TVB-N values of ground beef samples were expressed as mg/100 g.

Measurement of TBARS Value

A method used by Wang et al. (2020) was used in this work to measure the thiobarbituric acid reactive substance (TBARS). The absorbance values were recorded 532 and 600 nm and used to calculate TBARS value (mg malondialdehyde (MDA)/kg).

Statistical Analysis

All experiments and determinations were carried out in triplicate and the results were expressed as mean ± standard deviation (SD). Differences between mean values were established using Duncan's new multiple range tests at a confidence level of 95%. Statistical analysis was performed using SPSS version 22.0 (SPSS Inc., Chicago, IL, USA).

Results and Discussion

Influence of pH Variations on the Formation of Complex Coacervation

Complex coacervation, a typical process of electrostatic interaction between two biopolymers with opposite charge, can occur under controlled conditions within a typically narrow pH range. The degree of complex coacervation and the strength of electrostatic interaction between two biopolymers during the coacervate formation process can be significantly affected by the pH value (Bastos et al., 2020a). Therefore, pH optimization is essential to achieve the best condition for the complex coacervation process between PPI and NaAlg. The zeta potential and turbidity values of the PPI-NaAlg solutions between pH 2.0 and 7.0 were applied to estimate the optimal pH value for complex coacervation. Zeta potential of PPI ranged from − 32.20 to 28.07 mV in the pH range of 2.0 to 7.0 (Fig. 1A). This can be attributed to the amphoteric characteristics of PPI due to the presence of -NH_2 and -COOH (Timilsena et al., 2016). The isoelectric point (pI) of PPI was found to be about pH 4.9, as indicated by the close to 0 mV zeta potential. This value is close to the pI value of 5.0 reported by Zhao et al. (2021a, b). Within the testing pH range, the NaAlg solution was always negatively charged (Fig. 1A). Hence, complex coacervation between PPI and NaAlg would occur below pH of 4.9 due to the opposite charge of these two biopolymers.

The charge zeta potential values of mixed PPI-NaAlg solutions at different mixing ratios (PPI:NaAlg = 1:1, 2:1, 4:1, 6:1, and 8:1, w/w), as a response to the variation of pH, are presented displayed in Fig. 1B. A charge-neutral state (zeta potential = 0) in these PPI-NaAlg mixed systems was observed between pH 3.0 and 4.5 at which the highest degree of complex coacervate was expected to occur due to the strong electrostatic attraction between PPI and NaAlg (Timilsena et al., 2016). It was also observed that the pH of the charge neutral state shifted to higher pH values when the PPI-to-NaAlg ratio increased. This could be explained by the presence of excess amount of PPI above the amount required to saturate NaAlg in terms of electrostatic interactions (Bastos et al., 2020a; Chen et al., 2021; Timilsena et al., 2016). These findings suggest that the formation of complex coacervate between PPI and NaAlg at tested mixing ratios would occur between pH 3.0 and 4.5.

The change in turbidity of PPI-NaAlg mixtures at various mixing ratios as a response to pH change was determined to further confirm the optimal pH value for complex coacervation. The turbidity of the mixed suspensions increased with the decrease of the pH value when the pH was above pI (Fig. 1C). The suspensions became more or less transparent when the pH decreased well below the pI due to the dissolution of the coacervates. This observation indicated the fact that the complex coacervation occurs in a narrow pH range and is a reversible process. The highest turbidity values for PPI-NaAlg systems with PPI to NaAlg ratios of 1:1, 2:1, 4:1, 6:1, and 8:1 (w/w) were observed at pH of 3.1, 3.2, 3.6, 3.8, 4.0, and 4.1 which is around the pI of the PPI-NaAlg systems. Milošević et al. (2020) also reported that the optimum pH for the formation of complex coacervation was around the pI of the protein-fiber system.

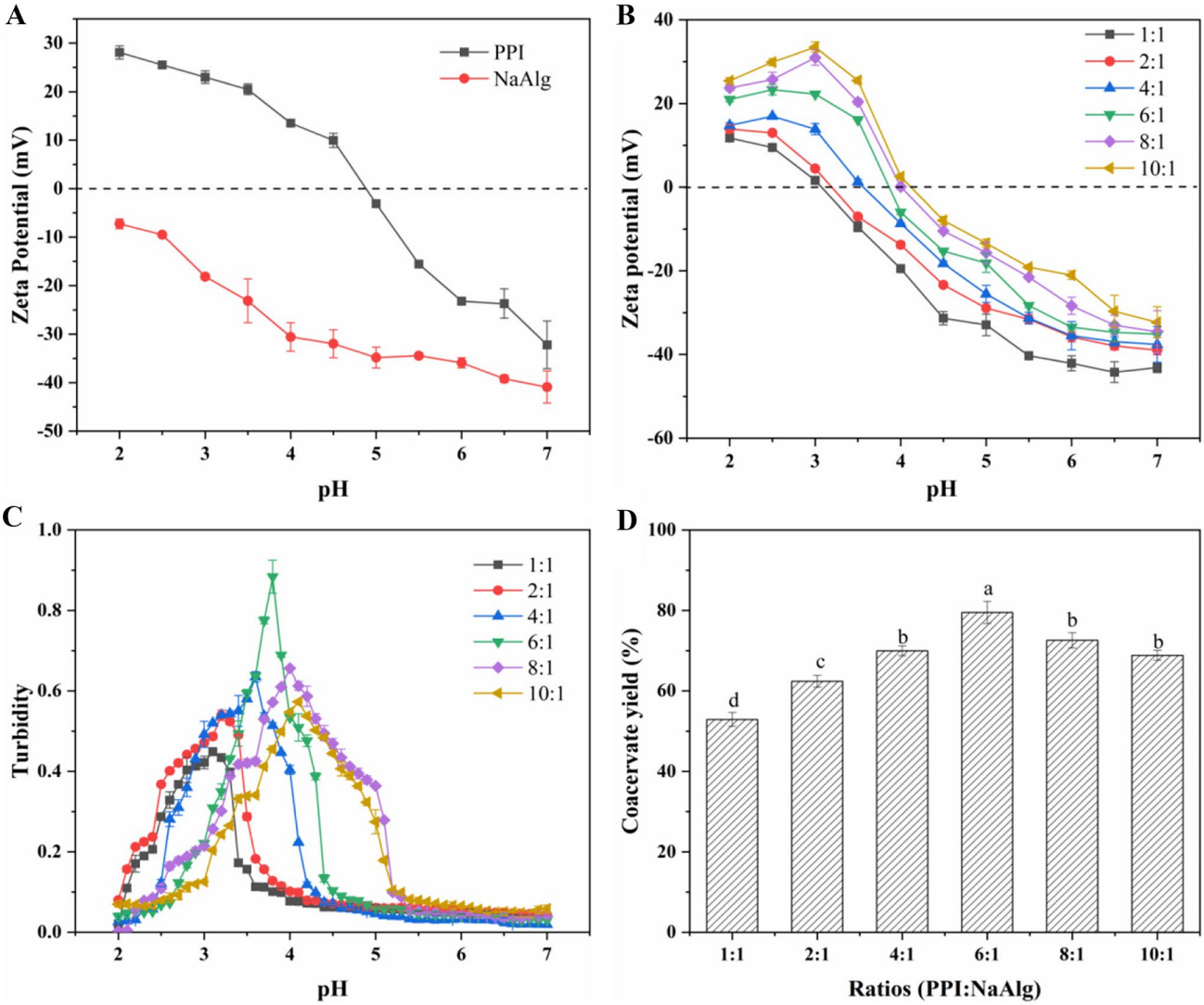

Fig. 1 The effects of pH and PPI/NaAlg mixing ratio on the formation of PPI-NaAlg complex coacervates. Zeta potential of PPI and NaAlg solutions (**A**). Zeta potential of different PPI-NaAlg systems (**B**). Turbidity of different PPI-NaAlg systems with the variation of pH (**C**). The coacervate yield of different PPI-NaAlg systems at the optimum pH value (**D**)

Influence of PPI-to-NaAlg Ratio on the Formation of Complex Coacervation

The mixing ratio is another determining parameter affecting the complex coacervation process. Turbidity and coacervate yield are considered two important indicators for confirming the optimum mixing ratio between protein and polysaccharides. As shown in Fig. 1C, the maximum turbidity was observed at the PPI-to-NaAlg mixing ratio of 6:1. The reason for the lower turbidity at mixing ratio of 1:1, 2:1, and 4:1 may be due to the excess negative charge and also steric repulsion caused by the excess amount of NaAlg. On the other hand, higher PPI-to-NaAlg ratios (8:1 and 10:1) would have increased the interaction among protein molecules, thus decreasing the turbidity (Naderi et al., 2020).

The yield of coacervate at different PPI-to-NaAlg ratios is presented in Fig. 1D. The mixing ratio of biopolymers significantly ($P<0.05$) affected the yield of complex coacervate. The coacervate yield as a function of PPI to NaAlg ratios followed the trend observed in turbidity data (Fig. 1C). The highest coacervate yield (79.50%) was observed at the PPI-to-NaAlg ratio of 6:1 (pH 3.8). On the basis of turbidity, zeta potential, and coacervate yield, the optimal parameters for the fabrication of PPI-NaAlg coacervates were PPI-to-NaAlg ratio of 6:1 and pH 3.8.

Characterization of PPI-NaAlg Coacervates and Microcapsules Containing REO

The particle diameter and micromorphology of PPI-NaAlg coacervates and REO microcapsules formed under the optimal conditions (PPI-to-NaAlg ratio = 6:1, pH = 3.8) before drying are displayed in Fig. 2. From Fig. 2, the complex coacervates of PPI-NaAlg processed an average particle diameter of 22.45 μm with an irregular network structure (Fig. 2A and B). Multicore structure (Fig. 2C) was observed in REO microcapsules indicating REO was successfully encapsulated. It was reported that microcapsules with multicore structure are superior to single-core ones in terms of mechanical strength, release properties, and thermal stability (Bylaitë et al., 2001). Meanwhile, the incorporation of REO into the complex coacervates increased the particle size from 22.45 to 33.43 μm (Fig. 2A). The increased particle size of REO microcapsules can be attributed to the interaction between core and wall materials altered the shape and particle size. These results are in accordance with earlier report on complex coacervates produced using sodium alginate and β-lactoglobulin (Bastos et al., 2020b).

The values of encapsulation efficiency, pay load, and encapsulation yield of the fabricated microcapsules containing REO were 89.80%, 53.17%, and 88.26% respectively (Fig. 2C). These results demonstrated that PPI-NaAlg complex coacervates could be successfully applied as the wall material to encapsulate REO.

FTIR Spectra Analysis

The structural characteristics of REO, PPI, NaAlg, and the interaction among them were investigated by FTIR analysis. As presented in Fig. 3, the band at 3298.91 cm^{-1} observed on the spectra of PPI could be correspond to the O–H and N–H stretching vibrations of free amino acid (Kord Heydari et al., 2021). The characteristic peaks located at 1238.74, 1538.56, and 1654.81 cm^{-1} could be resulted from the groups of C-H, N–H, and C = O in PPI molecules, respectively (Vera et al., 2020). The stretching vibration contributed by the C-H groups on the spectrum of PPI was appeared at 2960.94 and 1449.78 cm^{-1}.

As for NaAlg, the band appearing at 2927.05 and 3428.53 cm^{-1} could be related to the stretching vibration of C-H and O–H. Additionally, absorption peak found at 1615.69 cm^{-1} corresponds to CO_2^- present in carboxylic acid salts ($RCOO^-$). Similarly, the absorption band appearing at 1415.78 cm^{-1} could be due to C-O bond of the acid groups (RCOOH); the absorption bands appearing at 1031.23 and 1095.70 cm^{-1} assigned to the asymmetric vibrational stretch caused by C-O and C–O–C groups.

The interaction between PPI and NaAlg can also be demonstrated from the spectral data presented in Fig. 3. The typical absorption peak of uncomplexed NaAlg appearing at 1615.69 cm^{-1} disappeared on the FTIR spectra of PPI-NaAlg coacervates. Furthermore, the strong peaks of PPI at 3298.87 cm^{-1}, corresponding to O–H stretching vibration, shifted to 3293.91 cm^{-1} in PPI/NaAlg coacervates. These

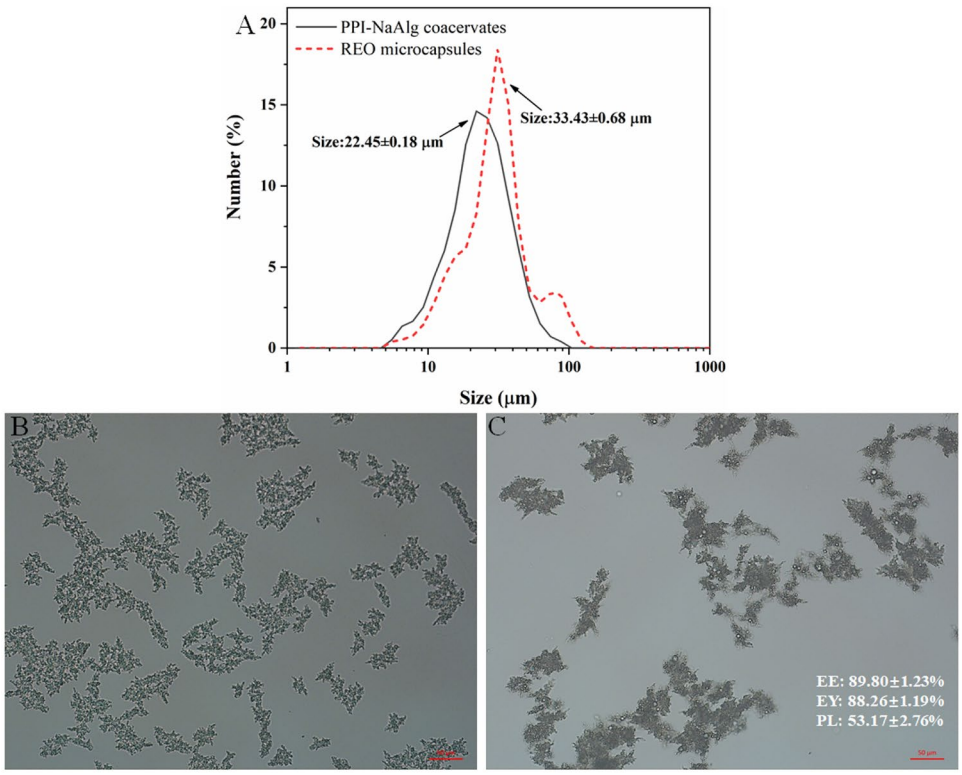

Fig. 2 Particle diameter analysis (**A**), morphology observation of PPI-NaAlg coacervates (**B**), and microcapsules containing REO (**C**)

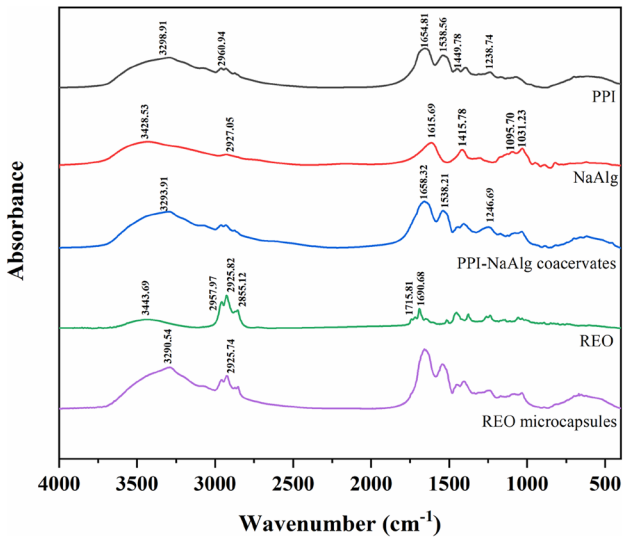

Fig. 3 FTIR spectra of PPI, NaAlg, PPI-NaAlg coacervates, REO, and REO microcapsules

results suggest the generation of hydrogen banding between O–H group of PPI molecules and C = O group of NaAlg molecules. Compared to uncomplexed PPI, the absorption peaks associated with amide I, II, and III bands shifted from 1654.89, 1538.56, and 1238.74 cm^{-1} to 1658.32, 1538.21, and 1246.69 cm^{-1}, respectively, in PPI-NaAlg complex coacervates, suggesting that electrostatic attraction had occurred between PPI and NaAlg (Li et al., 2021).

REO exhibited characteristic absorption peaks of C = C–C and O–H groups at 2957.97 and 3443.69 cm^{-1}, respectively (Fig. 3). The symmetric and asymmetric C-H stretching vibrations of methylene were presented as two absorption peaks appearing at 2855.12 and 2925.82 cm^{-1}, respectively. An intense absorption peak located at 1715.81 cm^{-1} on the spectrum of REO was corresponded to the existence of esters. The characteristic band observed in REO at 2925.74 cm^{-1} was also observed in REO microcapsules suggesting a successful microencapsulation of REO in PPI-NaAlg coacervates. In addition, the shift of the absorption bands of REO observed at 3443.69 cm^{-1} to 3290.54 cm^{-1} in REO microcapsules indicated the generation of hydrogen bond among the core and wall materials after microcapsulation (Duhoranimana et al., 2017).

Thermal Stability

The thermal stability of the tested samples was evaluated by thermogravimetric (TGA) analysis. The curves of differential thermogravimetric (DTG) and TGA of REO, PPI-NaAlg coacervates, and microcapsules with REO are displayed in Fig. 4. The data of TGA analysis of REO showed a mass reduction of 4.70% below 100 ℃ due to the evaporation of moisture and volatilization of REO (Duhoranimana et al., 2018; Zhang et al., 2021). Due to the boiling point of REO was reported to be about 275 °C (Xiao et al., 2019), the sharp mass loss of 79.51% of REO observed from TGA and DTG curves between 100and 200 ℃ may be attributed to the massive REO volatilization (Zhang et al., 2021).

A considerable weight loss (8.41%) of PPI-NaAlg coacervates was shown around 100 ℃ according to the TGA data due to the evaporation of water. A rapid thermal degradation of the PPI-NaAlg coacervates (55.46%) was noticed between 200 and 500 ℃. The pattern of weight loss in REO microcapsules

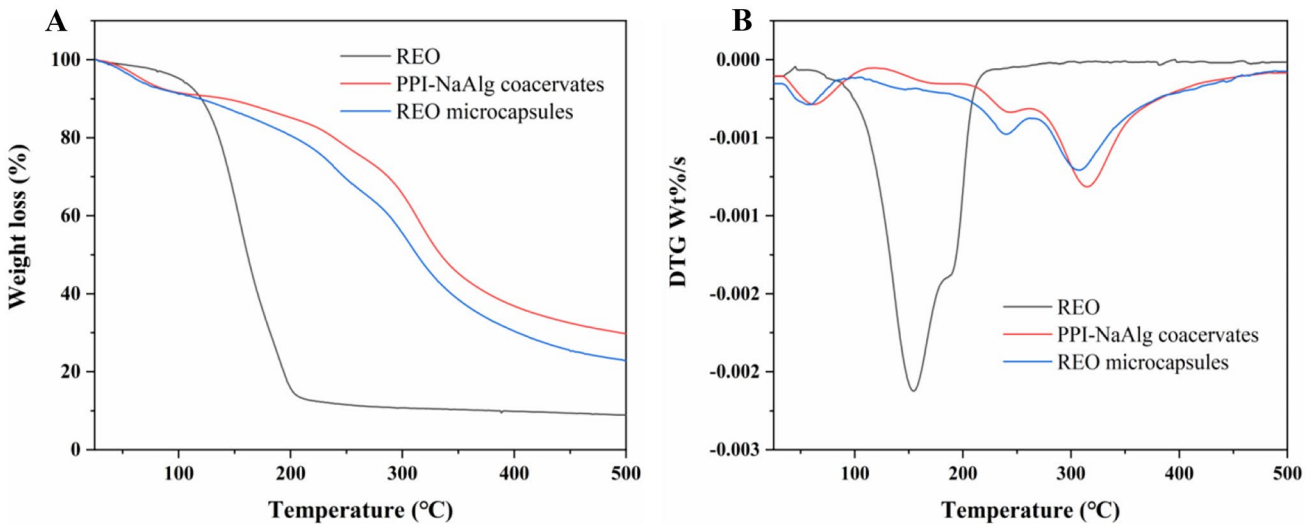

Fig. 4 The curves of **A** TGA and **B** DTG analysis of free REO, PPI-NaAlg coacervates, and microcapsules with REO

was similar to that in PPI-NaAlg coacervates; mass loss of 8.78% below 100 ℃ is related to the evaporation of moisture and unprotected REO. A rapid weight loss (57.69%) of the microcapsules occurred between 200 and 500 °C could be contributed by the breakdowns of wall materials, and the volatilization and degradation of the core materials (REO) have been unencapsulated. The findings indicate that the PPI-NaAlg complex coacervate shell matrix could enhance the thermal stability of free REO by microencapsulation technology. This finding is in agreement with several publications, for example, encapsulation of sesame oil in gelatin- gum Arabic complex coacervates (Dai et al., 2020), ginger essential oil in whey protein isolate-gum Arabic (Tavares & Noreña, 2020), and chia seed oil in chia seed protein-chia seed gum complex coacervates (Dai et al., 2020).

Release Characteristics of REO in Different Food Simulants

The REO release characteristics from PPI-NaAlg coacervates in four food models are displayed in Fig. 5A. As can be observed, REO was rapidly released within first 11 min in all food simulants with cumulative release percentage of 25.8%, 29.7%, 36.0, and 23.4% in aqueous, ethanol (10% and 50%, v/v) and acetic acid (3%, v/v) solutions, respectively. A sustained (slow) release behavior of REO from microcapsules was found in all solvents from 11 to 24 min, indicating its controlled release in these model foods. The highest cumulative release of REO was observed in 50% ethanol, followed by 10% ethanol, deionized water, and 3% acetic acid solutions.

This observation was in accordance with the findings of Bastos et al. (2020b), who used β-lactoglobulin/NaAlg for the microencapsulation of black pepper oil. Conversely, Chen et al. (2021) found that eugenol loaded microcapsules prepared using quinoa protein and gum Arabic as wall materials were most stable in water, followed by 10% ethanol, 3% acetic acid, and 50% ethanol. According to Muhoza et al. (2019), the multinuclear structure of the microcapsules prepared and the molecular/viscosity of the wall materials could affect the release characteristics of the core materials. Therefore, the different release rate of REO in food models could be due to the difference of wall materials, which play a principal role in the release characteristics of REO (core) (Qiu et al., 2022). REO exhibits poor solubility in water for its lipophilic nature, leading to the lower release rate of REO in aqueous solution (deionized water) compared to 10% and 50% ethanol solutions (Mahajan & Pal, 2020). Furthermore, the pH of the solution with acetic acid (3%, v/v) is about 4.3, which is closer to the isoelectric point (pH = 3.8) of the PPI-NaAlg system compared to other solutions, thus playing protective effects on the microcapsules containing REO owing to the stronger electrostatic interaction among PPI and NaAlg molecules at this pH.

The release profiles of the encapsulated REO were further fitted by Weibull model to gain insight on the release mechanism of REO from microcapsules. As shown in Fig. 5B, the release profile of REO from microcapsules in four different simulants fitted well by the Weibull model with correlation coefficient (R^2) of 0.99. As previously reported, $\beta \leq 0.75$ suggests that the release mechanism is Fickian diffusion; $0.75 < \beta \leq 1$ suggests the presence of swelling release behavior and diffusion, also recognized

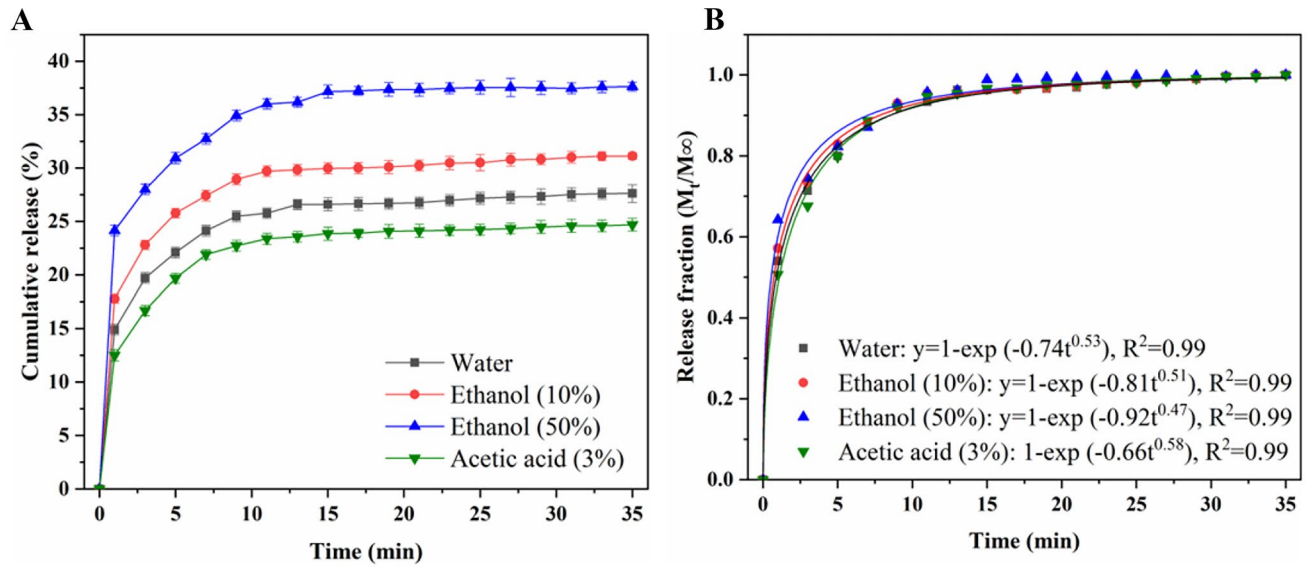

Fig. 5 Cumulative release curves of encapsulated REO (**A**) and release data of encapsulated REO fitted to Weibull model (**B**)

as non-Fickian diffusion (Macheras & Dokoumetzidis, 2000). According to Fig. 5B, the β value of the Weibull model fell between 0.47 and 0.58, indicating that the main release mechanism of REO from PPI/NaAlg coacervates in all food models occurred as a result of Fickian diffusion. Therefore, the swelling of the microcapsules can be neglected at this process. This phenomenon may be attributed to the poor swelling ability of the shell materials in these food simulants and the gradual diffusion of REO in these solutions.

Effect of REO and REO Microcapsules on E. coli and S. aureus

The effects of REO or REO microcapsules on the growth curves of *E. coli* (a gram-negative) *and S. aureus* (gram-positive) bacterial strains are presented in Fig. 6. A logarithmic growth was observed for both *E. coli* and *S. aureus* strains in the first 12 h followed by a slow growth stage (12–16 h). The OD_{600} value remained almost unchanged or even slightly decreased in the later stage of culture due to the lack of nutrients. In addition, the growth of *E. coil* and *S. aureus* was significantly restricted by the presence of REO, and the encapsulated REO displayed stronger inhibitory effect against these two bacteria compared to free REO. This phenomenon may be contributed by the slow-release behavior of the REO encapsulated in the microcapsules, which extend the action time of REO. Moreover, the growth of *E. coil* in the presence of REO or REO microcapsules was much higher than that of *S. aureus*, indicating that *S. aureus* was more sensitive to REO. This result is in accordance with those of Kang et al. (2022), who reported that REO showed a stronger inhibition effect on *S. aureus* than on *E. coil*. This may be attributed to the cell membrane difference of these bacteria strains (Cui et al., 2019).

Preservative Effect of REO Microcapsule on Ground Beef During Storage

TBC and TVB-N Analysis

Bacterial contamination is one of the most significant foodborne hazards in fresh meat products that affect public health (Zhao et al., 2020a, b). The change of TBC in ground beef during cold storage is shown in Fig. 7A. Although the TBC of all samples increased, the ground beef samples containing REO microcapsules showed the lowest growth TBC during cold storage. It further confirmed that REO microcapsules imparted sustained release effect on REO which prolonged its antibacterial properties. The TBC of the control samples on the 6th day was 6.4 $\log_{10}$ CFU/g, which exceeded the safety standard (6.0 $\log_{10}$ CFU/g) (Wan et al., 2020). This finding agreed with that of Mitsumoto et al. (2005), who reported that the shelf-life of fresh ground beef samples at 4 ℃ was about 7 days. Our ground beef samples containing REO and REO microcapsules had acceptable TBC values (TBC < 6.0 $\log_{10}$ CFU/g) up to 9 days of storage indicating to a good degree of antibacterial effects.

TVB-N is an important indicator for accessing freshness or shelf-life of meat/meat products (Huang et al., 2014). The microbial and enzymatic spoilage of proteins or other nitrogenous substances in meat are two main reasons for the production of TVB-N (Guo et al., 2021). Based on the Chinese Standard (GB/5009.228–2016), the TVB-N contents in fresh meat/meat products should not exceed 15 mg/100 g. As shown Fig. 7B, the values of TVB-N of ground beef samples increased in varying amount during storage. The control group showed a rapidly increasing trend of TVB-N value with the storage time reaching 16.38 mg/100 g at the

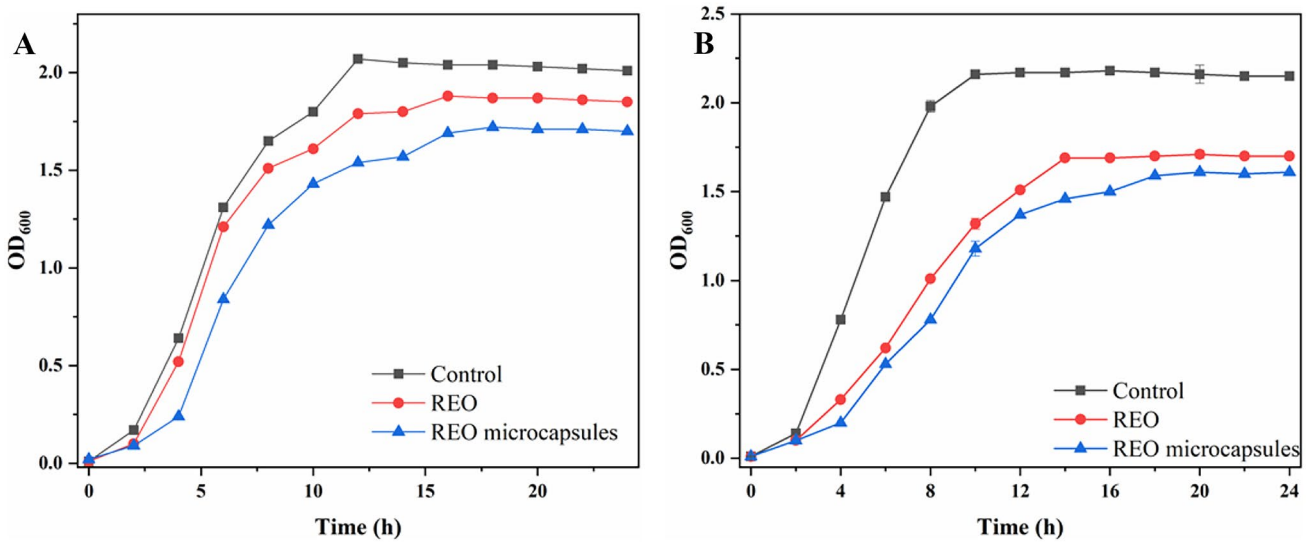

Fig. 6 Growth curves of *Escherichia coli* (**A**) and *Staphylococcus aureus* (**B**) with the presence of REO and REO microcapsules

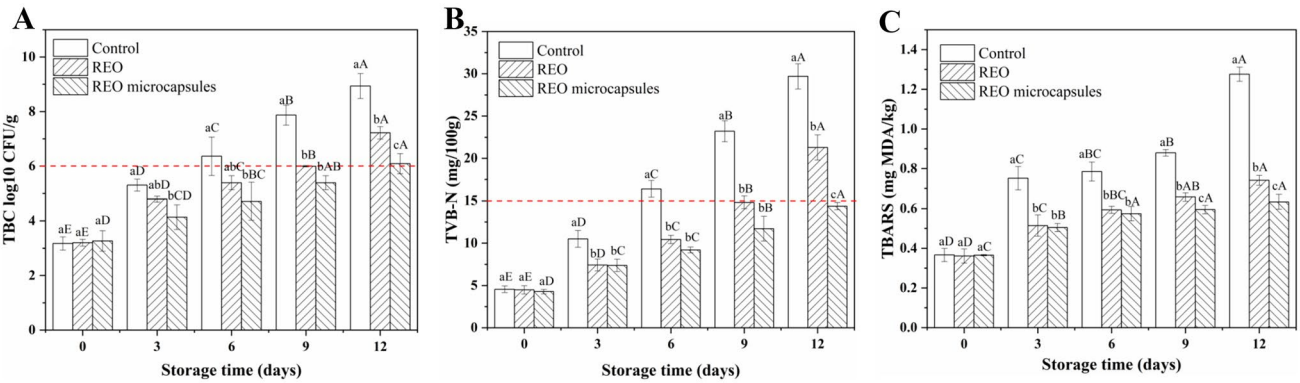

Fig. 7 The changes of **A** TBC, **B** TVB-N, and **C** TBRAS values of ground beef during cold storage (4 ℃). Note: Columns with different lowercase letters and different uppercase letters indicate significant difference ($P < 0.05$) among different samples at the same day and significant difference ($P < 0.05$) among the same ground beef samples at different storage periods, respectively

6th day due to the growth and reproduction of spoilage bacteria (Fig. 7A) and higher activity of endogenous enzyme (Chen et al., 2020). The values of TVB-N of the ground beef products treated with REO and REO microcapsules on the 9th (12th) day were 14.81 mg/100 g (21.28 mg/100 g) and 11.71 mg/100 g (14.36 mg/100 g), suggesting that the shelf-life of the refrigerated ground beef was prolonged to 9 and 12 days, by REO and REO microcapsules, respectively. These results show that REO microcapsules can prolong the shelf life of ground beef more effectively ($P < 0.05$) than REO.

TBARS Analysis

TBARS is an implicit indicator for measuring the degree of lipid peroxidation in meat products as it measures the malondialdehyde content produced from the oxidative decomposition of meat fat (Sun et al., 2021). An improvement of TBARS values was noticed in all beef products during 12 days of storage (Fig. 7C). Generally, the TBARS of the tested samples was around 0.36 mg MDA/kg of ground beef samples. The TBARS values of the samples without treatment was significantly higher ($P < 0.05$) compared to other samples in the entire storage period (3–12 days), suggesting that the degree of fat oxidation in the control samples was the highest. The ground beef samples containing REO microcapsules showed the lowest level of increase of TBARS value (0.63 mg MDA/100 g) at the end of storage than that of untreated sample (1.28 mg MDA/100 g) and sample containing free REO (0.74 mg MDA/100 g). These results showed that the oxidation of lipid in beef could be suppressed by incorporating of REO and REO microcapsule (Fernández-Pan et al., 2014).

Conclusion

The objective of this research was to obtain the optimum condition of the complex coacervation process occurring among PPI and NaAlg, use the PPI-NaAlg complex coacervates to produce REO microcapsules, and finally use these microcapsules, as preservative, to prolong the shelf-life of the ground beef samples. PPI-to-NaAlg ratios of 6:1 and pH 3.8 were found to be the optimum parameters for the preparation of these complex coacervates. REO microcapsules showed multinuclear structures with a particle size of 33.43 μm. Electrostatic interactions between PPI and NaAlg as well as hydrogen bonds among the wall matrix and REO (core) were found to be main molecular level interactions. The dried REO microcapsule had high encapsulation efficiency (89.80%), encapsulation yield (88.26%), and payload (53.17%). Microencapsulation of REO improved its thermal stability as indicated by the increase of degradation temperature from 100–200 ℃ to 200–500 ℃. REO microcapsules also displayed good sustained-release profile in model foods. A more effective inhibition of *E. coil* and *S. aureus* strains was achieved by REO microcapsules compared to free REO. REO microcapsules showed better antibacterial and antioxidant capacities compared to free REO when used as preservative in ground beef as indicated by the lower TBC, TVB-N, and TBARS values during storage. These results provide valuable information for preparing REO microcapsules using PPI-NaAlg complex coacervates and using these coacervates as preservatives for extending the shelf-life of ground beef. Our research provides an alternative path way for comprehensive utilization of PPI. In addition, the study also offers valuable information on the development of microcapsules with natural antibacterial and antioxidant substances for the preservation of meat products.

Author Contribution Liqing Qiu for investigation, conceptualization, software, and writing-original draft. Min Zhang for supervision, funding acquisition, writing-reviewing and editing and project administration. Benu Adhikari for writing-reviewing and editing. Lu Chang for supervision and resources.

Funding This work was supported by the National Natural Science Foundation Program of China (No. 31872902), Jiangsu Province Key Laboratory Project of Advanced Food Manufacturing Equipment and Technology (No. FMZ202003), the Postgraduate Research & Practice Innovation Program of Jiangsu Province (KYCX21_2050), and the Jinan City Science & Technology Innovation Project of Ten Agricultural Characteristic Industries.

Data Availability The data used to support the findings of this study are available from the corresponding author upon request.

Declarations

Conflict of Interest The authors declare no competing interests.

References

Bakry, A. M., Huang, J., Zhai, Y., & Huang, Q. (2019). Myofibrillar protein with κ- or λ-carrageenans as novel shell materials for microencapsulation of tuna oil through complex coacervation. *Food Hydrocolloids, 96*, 43–53.

Bansal, M., Dhowlaghar, N., Nannapaneni, R., Kode, D., Chang, S., Sharma, C. S., & Kiess, A. (2021). Decreased biofilm formation by planktonic cells of Listeria monocytogenes in the presence of sodium hypochlorite. *Food Microbiology, 96*, 103714.

Bastos, L. P. H., dos Santos, C. H. C., de Carvalho, M. G., & Garcia-Rojas, E. E. (2020a). Encapsulation of the black pepper (*Piper nigrum* L.) essential oil by lactoferrin-sodium alginate complex coacervates: Structural characterization and simulated gastrointestinal conditions. *Food Chemistry, 316*, 126345.

Bastos, L. P. H., de Sá Costa, B., Siqueira, R. P., & Garcia-Rojas, E. E. (2020b). Complex coacervates of β-lactoglobulin/sodium alginate for the microencapsulation of black pepper (*Piper nigrum* L.) essential oil: Simulated gastrointestinal conditions and modeling release kinetics. *International Journal of Biological Macromolecules, 160*, 861–870.

Bastos, L. P. H., Vicente, J., dos Santos, C. H. C., de Carvalho, M. G., & Garcia-Rojas, E. E. (2020c). Encapsulation of black pepper (*Piper nigrum* L.) essential oil with gelatin and sodium alginate by complex coacervation. *Food Hydrocolloids. 102*, 105605.

Bajac, J., Nikolovski, B., Lončarević, I., Petrović, J., Bajac, B., Đurović, S., & Petrović, L. (2022). Microencapsulation of juniper berry essential oil (*Juniperus communis* L.) by spray drying: Microcapsule characterization and release kinetics of the oil. *Food Hydrocolloids, 125*, 107430.

Bylaitë, E., Rimantas Venskutonis, P., & Maþdþierienë, R. (2001). Properties of caraway (*Carum carvi* L.) essential oil encapsulated into milk protein-based matrices. *European Food Research and Technology, 212*(6), 661–670.

Chen, F., Li, S., Zhong, G., & Liu, Y. (2020). Properties of novel chitosan incorporated with hexahydro-β-acids edible films and its effect on shelf life of pork. *Journal of Food Science, 85*(4), 947–955.

Chen, K., Zhang, M., Mujumdar, A. S., & Wang, H. (2021). Quinoa protein-gum Arabic complex coacervates as a novel carrier for eugenol: Preparation, characterization and application for minced pork preservation. *Food Hydrocolloids, 120*, 106915.

Cui, H., Zhang, C., Li, C., & Lin, L. (2019). Antibacterial mechanism of oregano essential oil. *Industrial Crops and Products, 139*, 111498.

da Silva Soares, B., de Carvalho, C. W. P., & Garcia-Rojas, E. E. (2021). Microencapsulation of sacha inchi oil by complex coacervates using ovalbumin-tannic acid and pectin as wall materials. *Food and Bioprocess Technology, 14*(5), 817–830.

Dai, H. H., Li, X. D., Wei, A. C., Wang, X. D., & Wang, D. Y. (2020). Characterization and oxidative stability of cold-pressed sesame oil microcapsules prepared by complex coacervation. *Journal of Oleo Science, 69*(7).

Duhoranimana, E., Karangwa, E., Lai, L., Xu, X., Yu, J., Xia, S., & Habinshuti, I. (2017). Effect of sodium carboxymethyl cellulose on complex coacervates formation with gelatin: Coacervates characterization, stabilization and formation mechanism. *Food Hydrocolloids, 69*, 111–120.

Duhoranimana, E., Yu, J., Mukeshimana, O., Habinshuti, I., Karangwa, E., Xu, X., & Zhang, X. (2018). Thermodynamic characterization of gelatin–sodium carboxymethyl cellulose complex coacervation encapsulating conjugated linoleic acid (CLA). *Food Hydrocolloids, 80*, 149–159.

Faidi, A., Lassoued, M. A., Becheikh, M. E. H., Touati, M., Stumbé, J.-F., & Farhat, F. (2019). Application of sodium alginate extracted from a Tunisian brown algae *Padina pavonica* for essential oil encapsulation: Microspheres preparation, characterization and in vitro release study. *International Journal of Biological Macromolecules, 136*, 386–394.

Fernández-Pan, I., Carrión-Granda, X., & Maté, J. I. (2014). Antimicrobial efficiency of edible coatings on the preservation of chicken breast fillets. *Food Control, 36*(1), 69–75.

Gomez-Estaca, J., Comunian, T. A., Montero, P., & Favaro-Trindade, C. S. (2018). Physico-chemical properties, stability, and potential food applications of shrimp lipid extract encapsulated by complex coacervation. *Food and Bioprocess Technology, 11*(8), 1596–1604.

Guo, Z., Ge, X., Gou, Q., Yang, L., Han, M., Han, G., & Han, L. (2021). Changes in chilled beef packaged in starch film containing sea buckthorn pomace extract and quality changes in the film during super-chilled storage. *Meat Science, 182*, 108620.

Göktepe, S., Ocak, B., & Özdestan-Ocak, Ö. (2021). Physico-chemical, sensory, and antioxidant characteristics of olive paste enriched with microencapsulated thyme essential oil. *Food and Bioprocess Technology, 14*(11), 2032–2045.

Huang, L., Zhao, J., Chen, Q., & Zhang, Y. (2014). Nondestructive measurement of total volatile basic nitrogen (TVB-N) in pork meat by integrating near infrared spectroscopy, computer vision and electronic nose techniques. *Food Chemistry, 145*, 228–236.

Jadach, B., Świetlik, W., & Froelich, A. (2022). Sodium alginate as a pharmaceutical excipient: Novel applications of a well-known polymer. *Journal of Pharmaceutical Sciences, 111*(5), 1250–1261.

Jawanda, S. K., Kafrani, R. S., & Ramaswamy, H. (2022). Tracking mustard slurry allergen reactivity through stove top cooking and enhanced thermal treatments using sandwich ELISA. *Food and Bioprocess Technology, 15*(4), 806–820.

Kord Heydari, M., Assadpour, E., Jafari, S. M., & Javadian, H. (2021). Encapsulation of rose essential oil using whey protein concentrate-pectin nanocomplexes: Optimization of the effective parameters. *Food Chemistry, 356*, 129731.

Karagozlu, M., Ocak, B., & Özdestan-Ocak, Ö. (2021). Effect of tannic acid concentration on the physicochemical, thermal, and antioxidant properties of gelatin/gum Arabic–walled microcapsules containing *Origanum onites* L. *Essential Oil. Food and Bioprocess Technology, 14*(7), 1231–1243.

Karimifar, P., Saei-Dehkordi, S. S., & Izadi, Z. (2022). Antibacterial, antioxidative and sensory properties of *Ziziphora*

clinopodioides-Rosmarinus officinalis essential oil nanoencapsulated using sodium alginate in raw lamb burger patties. *Food Bioscience., 47*, 101698.

Kang, Y., Wu, K., Sun, J., Liu, C., Su, C., & Yi, F. (2022). Preparation of Kushui Rose (*Rosa setate* x *Rosa rugosa*) essential oil fractions by double molecular distillation: Aroma and biological activities. *Industrial Crops and Products, 175*, 114230.

Li, F., Wang, H., & Mei, X. (2021). Preparation and characterization of phytosterol-loaded microcapsules based on the complex coacervation. *Journal of Food Engineering, 311*, 110728.

Liu, Q., Zhang, M., Bhandari, B., Xu, J., & Yang, C. (2020). Effects of nanoemulsion-based active coatings with composite mixture of star anise essential oil, polylysine, and nisin on the quality and shelf life of ready-to-eat Yao meat products. *Food Control, 107*, 106771.

Liu, X., Chen, L., Kang, Y., He, D., Yang, B., & Wu, K. (2021). Cinnamon essential oil nanoemulsions by high-pressure homogenization: Formulation, stability, and antimicrobial activity. *LWT-Food Science and Technology, 147*, 111660.

Macheras, P., & Dokoumetzidis, A. (2000). On the heterogeneity of drug dissolution and release. *Pharmaceutical Research, 17*(2), 108–112.

Matricardi, P., Meo, C. D., Coviello, T., & Alhaique, F. (2008). Recent advances and perspectives on coated alginate microspheres for modified drug delivery. *Expert Opinion on Drug Delivery., 5*(4), 417–425.

Mahajan, M., & Pal, P. K. (2020). Flower yield and chemical composition of essential oil from Rosa damascena under foliar application of $Ca(NO_3)_2$ and seasonal variation. *Acta Physiologiae Plantarum, 42*(2), 23.

Milošević, M. M., Đorđević, T. R., & Antov, M. G. (2020). Complex coacervation of acid-extracted fiber from butternut squash (*Cucurbita moschata*) and protein. *Food Hydrocolloids, 108*, 105999.

Misra, S., Pandey, P., Dalbhagat, C. G., & Mishra, H. N. (2022). Emerging technologies and coating materials for improved probiotication in food products: A review. *Food and Bioprocess Technology, 15*(5), 998–1039.

Mitsumoto, M., O'Grady, M. N., Kerry, J. P., & Joe Buckley, D. (2005). Addition of tea catechins and vitamin C on sensory evaluation, colour and lipid stability during chilled storage in cooked or raw beef and chicken patties. *Meat Science, 69*(4), 773–779.

Muhoza, B., Xia, S., Cai, J., Zhang, X., Duhoranimana, E., & Su, J. (2019). Gelatin and pectin complex coacervates as carriers for cinnamaldehyde: Effect of pectin esterification degree on coacervate formation, and enhanced thermal stability. *Food Hydrocolloids, 87*, 712–722.

Naderi, B., Keramat, J., Nasirpour, A., & Aminifar, M. (2020). Complex coacervation between oak protein isolate and gum Arabic: Optimization & functional characterization. *International Journal of Food Properties, 23*(1), 1854–1873.

Plati, F., Ritzoulis, C., Pavlidou, E., & Paraskevopoulou, A. (2021). Complex coacervate formation between hemp protein isolate and gum Arabic: Formulation and characterization. *International Journal of Biological Macromolecules, 182*, 144–153.

Qiu, L., Zhang, M., Adhikari, B., & Chang, L. (2022). Microencapsulation of rose essential oil in mung bean protein isolate-apricot peel pectin complex coacervates and characterization of microcapsules. *Food Hydrocolloids, 124*, 107366.

Ren, X., Hou, T., Liang, Q., Zhang, X., Hu, D., Xu, B., & Ma, H. (2019). Effects of frequency ultrasound on the properties of zein-chitosan complex coacervation for resveratrol encapsulation. *Food Chemistry, 279*, 223–230.

Rodrigues Arruda, T., Fontes Pinheiro, P., Ibrahim Silva, P., & Campos Bernardes, P. (2022). Exclusive raw material for beer production? Addressing greener extraction techniques, the relevance, and prospects of hops (*Humulus lupulus* L.) for the food industry. *Food and Bioprocess Technology, 15*(2), 275–305.

Salvia-Trujillo, L., Rojas-Graü, M. A., Soliva-Fortuny, R., & Martín-Belloso, O. (2013). Effect of processing parameters on physicochemical characteristics of microfluidized lemongra**ss** essential oil-alginate nanoemulsions. *Food Hydrocolloids, 30*(1), 401–407.

Santos, M. B., Geraldo de Carvalho, M., & Garcia-Rojas, E. E. (2021). Carboxymethyl tara gum-lactoferrin complex coacervates as carriers for vitamin D3: Encapsulation and controlled release. *Food Hydrocolloids, 112*, 106347.

Smaoui, S., Ben Hlima, H., Ben Braïek, O., Ennouri, K., Mellouli, L., & Mousavi Khaneghah, A. (2021). Recent advancements in encapsulation of bioactive compounds as a promising technique for meat preservation. *Meat Science, 181*, 108585.

Stănciuc, N., Turturică, M., Oancea, A. M., Barbu, V., Ioniţă, E., Aprodu, I., & Râpeanu, G. (2017). Microencapsulation of anthocyanins from grape skins by whey protein isolates and different polymers. *Food and Bioprocess Technology, 10*(9), 1715–1726.

Sun, Y., Zhang, M., Bhandari, B., & Bai, B. (2021). Nanoemulsion-based edible coatings loaded with fennel essential oil/cinnamaldehyde: Characterization, antimicrobial property and advantages in pork meat patties application. *Food Control, 127*, 108151.

Tavares, L., Barros, H. L. B., Vaghetti, J. C. P., & Noreña, C. P. Z. (2019). Microencapsulation of garlic extract by complex coacervation using whey protein isolate/chitosan and gum Arabic/chitosan as wall materials: Influence of anionic biopolymers on the physicochemical and structural properties of microparticles. *Food and Bioprocess Technology, 12*(12), 2093–2106.

Tavares, L., & Noreña, C. P. Z. (2020). Encapsulation of ginger essential oil using complex coacervation method: Coacervate formation, rheological property, and physicochemical characterization. *Food and Bioprocess Technology, 13*(8), 1405–1420.

Timilsena, Y. P., Adhikari, R., Barrow, C. J., & Adhikari, B. (2016). Microencapsulation of chia seed oil using chia seed protein isolate chia seed gum complex coacervates. *International Journal of Biological MacromolecuLes, 91*, 347–357.

Ulusoy, S., Boşgelmez-Tınaz, G., & Seçilmiş-Canbay, H. (2009). Tocopherol, carotene, phenolic contents and antibacterial properties of rose essential oil, hydrosol and absolute. *Current Microbiology, 59*(5), 554.

Vera, A., Tapia, C., & Abugoch, L. (2020). Effect of high-intensity ultrasound treatment in combination with transglutaminase and nanoparticles on structural, mechanical, and physicochemical properties of quinoa proteins/chitosan edible films. *International Journal of Biological Macromolecules, 144*, 536–543.

Wan, J., Pei, Y., Hu, Y., Ai, T., Sheng, F., Li, J., & Li, B. (2020). Microencapsulation of eugenol through gelatin-based emulgel for preservation of refrigerated meat. *Food and Bioprocess Technology, 13*(9), 1621–1632.

Wang, Q., Zhang, L., & Ding, W. (2020). Eugenol nanocapsules embedded with gelatin-chitosan for chilled pork preservation. *International Journal of Biological Macromolecules, 158*, 837–844.

Xiao, Z., Kang, Y., Hou, W., Niu, Y., & Kou, X. (2019). Microcapsules based on octenyl succinic anhydride (OSA)-modified starch and maltodextrins changing the composition and release property of rose essential oil. *International Journal of Biological Macromolecules, 137*, 132–138.

Yang, J., Duan, Y., Geng, F., Cheng, C., Wang, L., Ye, J., Zhang, H., Peng, D., & Deng, Q. (2022). Ultrasonic-assisted pH shift-induced interfacial remodeling for enhancing the emulsifying and foaming properties of perilla protein isolate. *Ultrasonics Sonochemistry, 89*, 106108.

Zanin, R. C., Smrke, S., Yeretzian, C., Kurozawa, L. E., & Yamashita, F. (2021). Ultrasound-assisted emulsification of roasted coffee oil in complex coacervates and real-time coffee aroma release

by PTR-ToF–MS. *Food and Bioprocess Technology, 14*(10), 1857–1871.

Zhang, J., Jia, G., Wanbin, Z., Minghao, J., Wei, Y., Hao, J., & Sun, A. (2021). Nanoencapsulation of zeaxanthin extracted from Lycium barbarum L. by complex coacervation with gelatin and CMC. *Food Hydrocolloids, 112*, 106280.

Zhao, L., Zhang, M., Bhandari, B., & Bai, B. (2020a). Microbial and quality improvement of boiled gansi dish using carbon dots combined with radio frequency treatment. *International Journal of Food Microbiology, 334*, 108835.

Zhao, L., Zhang, M., Wang, H., & Devahastin, S. (2020b). Effect of carbon dots in combination with aqueous chitosan solution on shelf life and stability of soy milk. *International Journal of Food Microbiology, 326*, 108650.

Zhao, Q., Wang, L., Hong, X., Liu, Y., & Li, J. (2021a). Structural and functional properties of perilla protein isolate extracted from oilseed residues and its utilization in Pickering emulsions. *Food Hydrocolloids, 113*, 106412.

Zhao, Q., Yan, W., Liu, Y., & Li, J. (2021b). Modulation of the structural and functional properties of perilla protein isolate from oilseed residues by dynamic high-pressure microfluidization. *Food Chemistry, 365*, 130497.